JOURNAL OF CATALYSIS 145, 132–140 (1994)

Structure Characterization of Platinum/Alumina, Rhenium/Alumina, and Platinum–Rhenium/Alumina Catalysts

Chen Laiyuan, Ni Yueqin, Zang Jingling, Lin Liwu, Luo Xihui,* and Cheng Sen*

*Dalian Institute of Chemical Physics, Chinese Academy of Sciences, P.O. Box 110, Dalian 116023, China; and *Funshun Institute of Petroleum Chemical Engineering, SINOPEC, Funshun 113001, Liaoning, China*

Received March 4, 1993; revised June 18, 1993

The structures of Pt, Re, and Pt–Re catalysts supported on alumina containing 0.14 wt% titania were studied in the stages of impregnation, calcination, and reduction by UV diffuse reflectance spectroscopy (DRS), temperature-programmed reduction (TPR), selected area electron diffraction (SAED), and carbon monoxide and hydrogen adsorption measurements. Both platinum and rhenium species interacted strongly with the support after calcination. It is suggested that the platinum species interacts more strongly with titania than with alumina, while the converse is true with the rhenium species. A Pt_3Ti alloy was found in both the reduced Pt/Al_2O_3 and reduced $Pt–Re/Al_2O_3$ catalysts. An $Al(ReO_4)_3$ complex was found in the Re/Al_2O_3 catalyst which was reduced at 480°C. Pt(0), Re(0), and Pt_3Ti coexist in the reduced $Pt–Re/Al_2O_3$ catalyst and the surface concentration of Re(0) increases with the Re/Pt ratio. Hydrogen adsorption at a high temperature increases with increasing Re/Pt ratio. It is possible that this kind of hydrogen is responsible for the higher stability of the catalyst with a high Re/Pt ratio. © 1994 Academic Press, Inc.

INTRODUCTION

Bimetallic Pt–Re reforming catalysts have been widely used in the reforming industry since their introduction by Kluksdahl (1). There are many benefits from the addition of a second metal, rhenium, to Pt/Al_2O_3. It has been reported that there are platinum atoms, rhenium atoms, PtRe alloys (or clusters), and Re^{4+} ions in the reduced Pt–Re catalyst (2–6). Conversely, a fair number of investigators have argued that there is no PtRe alloy formation in the Pt–Re catalysts (7–10). The composition phases in the catalyst have not been clarified so far. Furthermore, there may be more complex species in this catalyst system because the metals are highly dispersed on alumina and there may exist strong metal–support interaction (SMSI), especially when titania is present in the support (11). Knowledge of the composition phases in the catalyst and the roles they play is very important in reforming practice because the interaction of these phases may have a profound effect on selectivity in reforming reactions. This is a study of the structures of these catalysts.

In the present work, we studied the structures of Pt/Al_2O_3, Re/Al_2O_3, and coimpregnated $Pt–Re/Al_2O_3$ catalysts. In order to understand the genesis of the structures of these catalysts, experiments were carried out in the stages of impregnation, calcination and reduction. The influence of the Re/Pt ratio on the structures of the Pt–Re catalysts is discussed. An understanding of Re/Al_2O_3 catalysts is also helpful to the operation of olefin metathesis.

EXPERIMENTAL

Catalyst Preparation

Gamma-Al_2O_3 containing 0.14 wt% titanium was used as the support. Its BET surface area is 204 m^2/g and its pore volume is 0.60 cm^3/g. All the catalysts were prepared by impregnating the gamma-Al_2O_3 with H_2PtCl_6, $HReO_4$, or their mixed solutions. After impregnation, the catalysts were dried at 120°C and calcined at 500°C in air for 4 hr. The catalysts were prepared as three groups. The first group was Pt/Al_2O_3 catalysts with different platinum contents, A1 : 0.15 wt%, A2 : 0.3 wt%, A3 : 0.5 wt%. The second group was a Re/Al_2O_3 catalyst (B) with 0.25 wt% rhenium. The third group was $Pt–Re/Al_2O_3$ catalysts. C1 : 0.15 wt% Pt–0.35 wt% Re, C2 : 0.15 wt% Pt–0.25 wt% Re, C3 : 0.3 wt% Pt–0.3 wt% Re, C4 : 0.5 wt% Pt–0.35 wt% Re, C5 : 0.5 wt%–0.25 wt%. The chloride content was 0.9 wt% on all of the catalysts.

UV Diffuse Reflectance Spectroscopy and TPR

Diffuse reflectance spectra of the catalysts were recorded with a Shimadzu UV-365 spectrometer in the wavelength range of 190–660 nm. The scan speed was 100 nm/min. Catalysts were pressed into tablets and dried at 120°C for 2 hr to remove water. The alumina support was used as reference. Temperature-programmed reduction was monitored in a reducing gas of 5% H_2/Ar with a heating rate of 12°C/min. The catalyst was crushed into 40 to 80 mesh powder before the TPR run. The amount of hydrogen consumption is calculated from the area un-

0021-9517/94 $5.00

der the TPR curves. The TPR curves were calibrated by reducing a known amount of pure CuO under the same TPR conditions.

Selected Area Electron Diffraction

The TEM used in this study was a Hitachi H-600 model transmission electron microscope. The catalysts were pretreated with HF aqueous solution after 480°C reduction in order to remove most of the alumina. Areas where particles were abundant were selected for diffraction. The interplanar spacings (d) of samples can be calculated according to the fundamental equation of electron diffraction, that is, $\lambda L = Rd$. A gold membrane was used as the standard sample for calculating the TEM camera constant. The total error of the calculated interplanar spacings (d) was about 0.02 Å, but the errors of some results may be higher because of poor definitions of the diffraction rings at some orientations.

Carbon Monoxide Adsorption Measurement

The CO adsorption isotherms of the catalysts were measured at 25°C using a static volumetric technique. Prior to the adsorption of CO, each sample was reduced in a flow of hydrogen at 480°C for 1 hr and in static hydrogen at 450°C for another hour. The sample was degassed for 4 hr to a final pressure of approximately 1.33×10^{-4} Pa. The CO adsorption pressure was increased from 6.6×10^3 to 5.05×10^4 Pa for the measurement. After the total adsorption amount was determined, the system was evacuated to remove weakly adsorbed CO. Another adsorption measurement then measured the physical adsorption of CO. Uptakes were determined by extrapolation to the Y-axis.

Hydrogen Adsorption Isobar Measurement

Hydrogen adsorption isobars were also measured in a static apparatus. The pretreatment of each sample was the same as described for the CO adsorption measurement. In the hydrogen adsorption measurement, the hydrogen pressure was maintained at about 6.6×10^3 Pa and the adsorption temperature varied from 0 to 450°C.

RESULTS

UV Diffuse Reflectance Spectra

The UV absorption results for the impregnated solutions are given in Table 1. The characteristic absorption bands of H_2PtCl_6 solution occur at 200, 260, and 355 nm, and those of the $HReO_4$ solution are at 203 and 226 nm. The diffuse reflectance spectra of calcined Pt/Al_2O_3 and Re/Al_2O_3 catalysts are given in Fig. 1.

When gamma-Al_2O_3 was impregnated with H_2PtCl_6, the

TABLE 1

The UV Characteristic Absorption Bands of H_2PtCl_6 and $HReO_4$ Solutions and Dried Pt/Al_2O_3 Catalyst

Sample	Absorption bands (nm)
H_2PtCl_6 solution	200, 260, 355
$HReO_4$ solution	203, 226
Dried Pt/Al_2O_3	275, 355, 450

$[PtCl_6]^{2-}$ anion adsorbed on the positive site of alumina. An adsorbed $[PtCl_6]^{2-}$ is slightly different from a free $[PtCl_6]^{2-}$ with absorption bands at 275,355, and 450 nm (Table 1). The first band is attributed to a charge transfer (CT) band (from Cl^- to Pt) and the latter two bands are d–d transition bands of platinum (12). After calcination, there are only two principal absorption bands at 230 and 350 nm (Fig. 1). The 350 nm band is almost unchanged because it is a d–d transition band of platinum. However, the charge transfer band at 275 nm shifts to 230 nm. This change must be due to a change in the environment of platinum. It thus allows us to assume that the platinum species interacts strongly with the support. It is also possible that the surface complex $[PtO_xCl_y]$ was formed (12). Moreover, because the absorption band of PtO_2 appears at 350 nm, although the presence of PtO_2 species in the Pt/Al_2O_3 catalyst is very possible, its presence cannot be deconvoluted.

The absorption bands of calcined Re/Al_2O_3 are quite different from those of a $HReO_4$ solution. The calcined

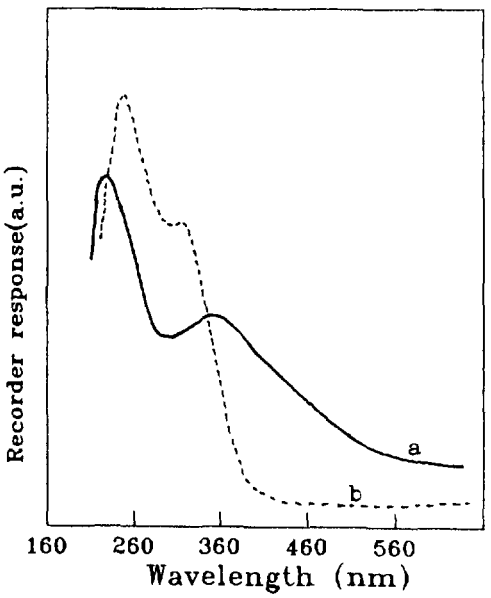

FIG. 1. Diffuse reflectance spectra of (a) calcined Pt/Al_2O_3 and (b) calcined Re/Al_2O_3 catalysts.

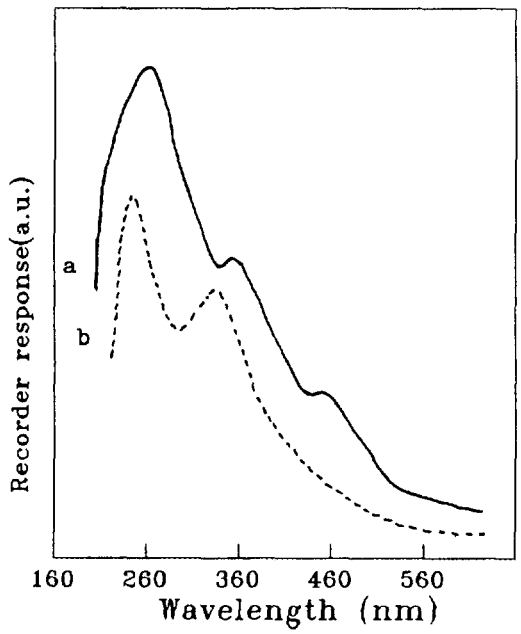

FIG. 2. Diffuse reflectance spectra of (a) uncalcined and (b) calcined C1 catalyst.

Re/Al_2O_3 has absorption bands at 240 and 305 nm (see Fig. 1), but the $HReO_4$ solution shows absorption bands at 203 and 226 nm. This result suggests that the chemical environment of rhenium in the Re/Al_2O_3 catalyst is greatly changed. The formation of a surface complex is possible. At the very least the symmetry of ReO_4^- is drastically altered.

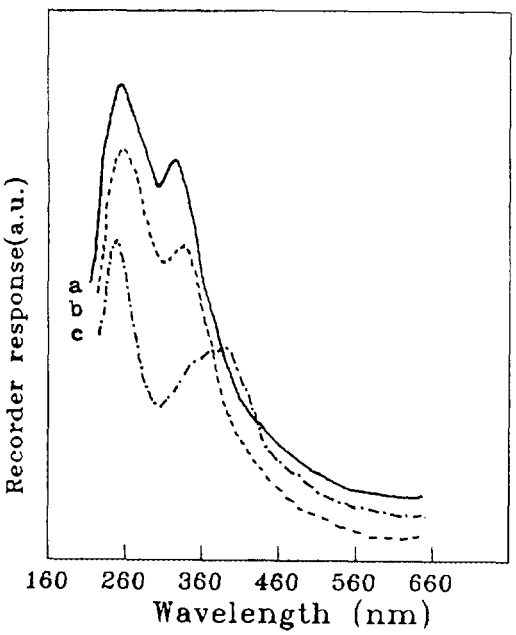

FIG. 3. Diffuse reflectance spectra of Pt–Re catalysts with different Re/Pt ratios: (a) Re/Pt = 2.33, (b) Re/Pt = 1.67, (c) Re/Pt = 1.

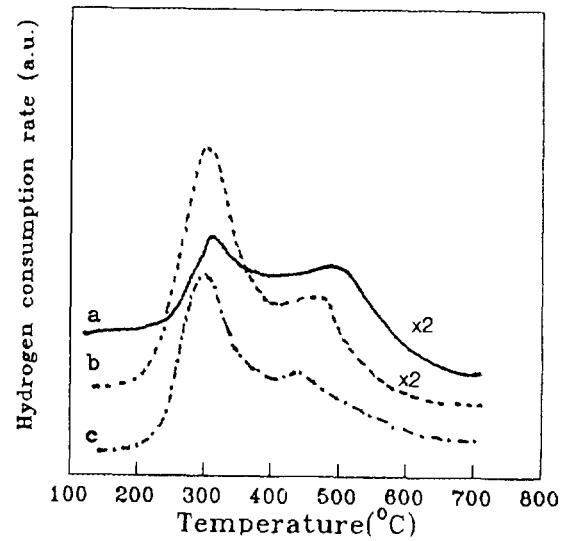

FIG. 4. TPR spectra of Pt/Al_2O_3 catalysts with different platinum contents: (a) 0.15 wt%, (b) 0.3 wt%, (c) 0.5 wt%.

The diffuse reflectance spectrum of a freshly impregnated Pt–Re catalyst with the composition shown for the C1 catalyst, which was dried but not calcined, is given in Fig. 2. Its absorption bands appear at 270, 350, and 450 nm. However, if the above catalyst was calcined at 500°C, it exhibits only two principal absorption bands at 245 and 330 nm (Fig. 2).

In order to study the influence of the Re/Pt ratio on the catalyst structure, a series of $Pt–Re/Al_2O_3$ catalysts with a Re/Pt ratio range of 1 to 2.33 were investigated. The results are shown in Fig. 3. It can be seen that if Re/Pt = 1, the diffuse reflectance features of the catalyst are like those of Pt/Al_2O_3. However, if Re/Pt > 1, the diffuse reflectance spectra resemble those of Re/Al_2O_3.

It should be noted that in the above analyses the presence of titanium was not taken into account. This is because a comparison of the DRS spectrum of pure alumina with that of the titania-containing alumina did not show any change in the DRS results under our experimental conditions.

Temperature-Programmed Reduction Studies

The TPR profiles of Pt/Al_2O_3 catalysts with different platinum contents are given in Fig. 4. The first peak is at about 300°C. The other peak changes from 435 to 475°C when the platinum content decreases from 0.5 to 0.15 wt%. From the hydrogen consumption in the TPR, the H_2/Pt ratio was always slightly greater than 1.

The TPR spectra of Re/Al_2O_3 and the support are shown in Fig. 5. The TPR profile of Re/Al_2O_3 illustrates that reduction of rhenium oxide species starts at about 430°C. Two maximum peaks occurred at 615°C and 740°C. The

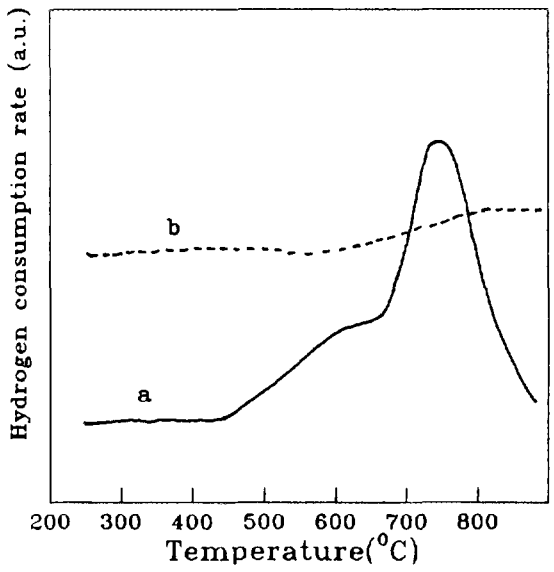

FIG. 5. TPR spectra of (a) Re/Al_2O_3 and (b) support.

TPR profile of the support in Fig. 5 shows that the support was not reduced until near 600°C.

Figure 6 gives the TPR spectra of $Pt–Re/Al_2O_3$ catalysts with different Re/Pt ratios. When Re/Pt is 0.5 (C5 catalyst), three reduction peaks at 300, 500, and 710°C were seen. A peak with a ramp tail at 300°C and a peak at 700°C were observed for the C3 catalyst. For the C1 catalyst,

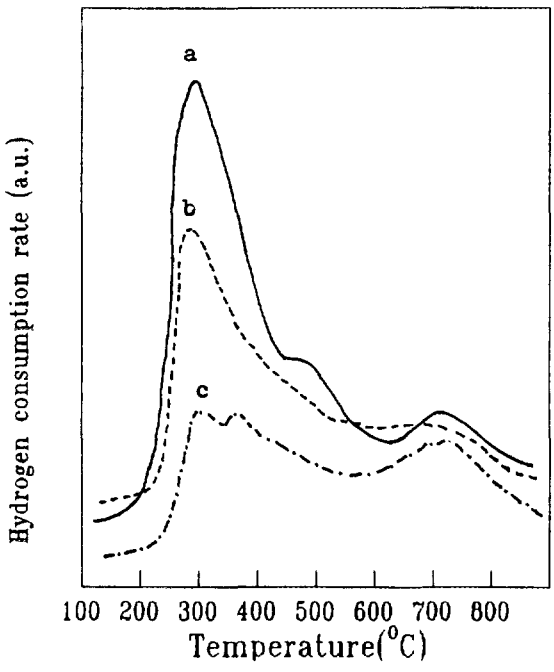

FIG. 6. TPR spectra of Pt–Re catalysts with different Re/Pt ratios: (a) Re/Pt = 0.5, (b) Re/Pt = 1, (c) Re/Pt = 2.33.

peaks at 300, 350, and 720°C were observed. The hydrogen consumption in the TPR for temperatures below 500°C ratioed to the metals, $H_2/(Pt + Re)$, was very near to 1, and this ratio decreased with the increasing of the Re/Pt ratio.

Selected Area Electron Diffraction Studies

The catalyst phases in the reduced catalysts were examined by means of selected area electron diffraction (SAED). The diffraction patterns are given in Fig. 7 and the calculated interplanar spacings are listed in Table 2. The specific interplanar spacings of certain Miller indices of standard compounds from ASTM data files are also listed in Table 2 to assist identification of the catalyst phases. By comparison of the experimental results to the standard interplanar spacings chosen from ASTM files, we found that a Pt_3Ti alloy was formed in both reduced Pt/Al_2O_3 and reduced $Pt–Re/Al_2O_3$ catalysts. Interestingly, $Al(ReO_4)_3$ complex was formed in the Re/Al_2O_3 catalyst. Metallic platinum and rhenium and a Pt_3Ti alloy were found in a Pt–Re catalyst (C4). We did not examine low platinum content bimetallic catalysts because of difficulty in seeing any diffraction.

CO Adsorption Studies

The data for CO isothermal adsorption at 25°C are given in Table 3. The amount of strongly adsorbed CO was obtained from the difference between the total adsorption and the weak adsorption. Corrections were made by the measurement of CO adsorption on the blank alumina. The amount of CO chemisorbed on Re/Al_2O_3 is very little. The CO adsorbed on the C1 catalyst was mainly the strongly adsorbed type while weakly adsorbed CO was predominant on the C4 catalyst. The ratio of strongly adsorbed CO molecules to platinum or rhenium atoms was calculated: CO/Pt was 0.54 for Pt/Al_2O_3 catalyst and CO/Re was 0.15 for Re/Al_2O_3 catalyst.

Hydrogen Adsorption Isobars

Figure 8 shows the isobars for hydrogen adsorption on the Pt/Al_2O_3 and Re/Al_2O_3 catalysts. The maximum uptake of hydrogen for Pt/Al_2O_3 is obtained at temperatures lower than 100°C. When the temperature increases from 0 to 450°C, the hydrogen uptake decreases from 39 to 23 ml/g Pt. Hydrogen adsorption hardly occurred on Re/Al_2O_3 when the temperature was lower than 100°C. However, it increased drastically at temperatures higher than 100°C.

Figure 9 gives the results of hydrogen isobars on two Pt–Re catalysts. The hydrogen uptake increased significantly with an increase in temperature for the catalyst with Re/Pt = 2.3. However, it changed only a little for the catalyst with Re/Pt = 0.5. Clearly, the hydrogen ad-

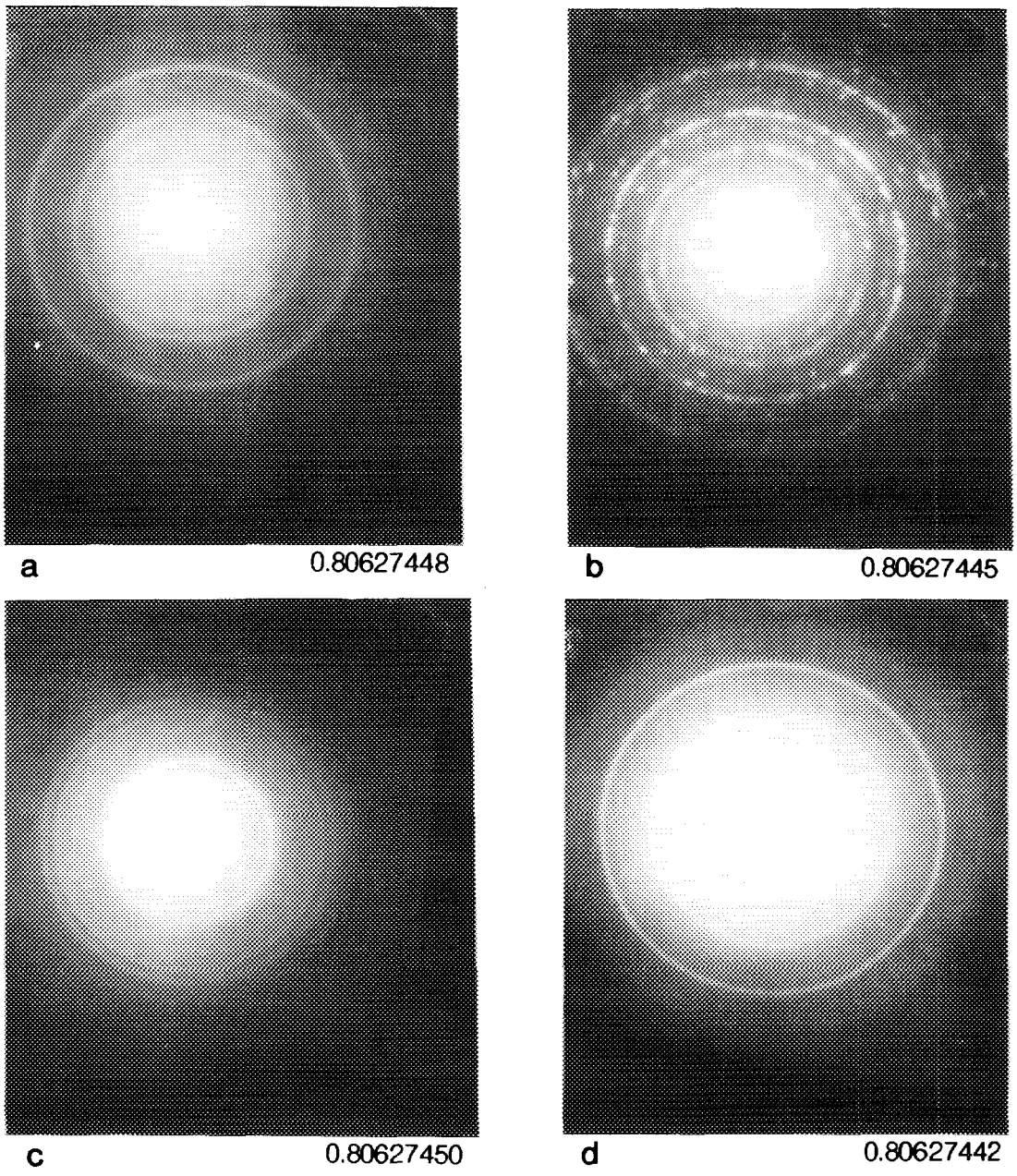

FIG. 7. Selected area electron diffraction patterns: (a) support, (b) Pt/Al_2O_3, (c) Re/Al_2O_3, (d) $Pt–Re/Al_2O_3$ (C4).

sorption features of the catalyst with Re/Pt = 2.3 are much like those of the Re/Al_2O_3 catalyst.

DISCUSSION

Pt/Al_2O_3 Catalyst

The UV absorption spectrum of H_2PtCl_6 solution shows three absorption bands at 200, 260, and 355 nm. The first two are attributed to charge transfer (CT) bands (13). Table 1 shows that the dried Pt/Al_2O_3 catalyst also has three absorption bands at 275, 355, and 450 nm. When the $[PtCl_6]^{2-}$ ion adsorbs on alumina, the 355 nm band (*d–d* band of platinum) did not change, the 200 nm band was not detected and a new *d–d* band at 450 nm appeared. The CT band at 260 nm shifted to 275 nm; this shift is regarded as the result of a chemical interaction of the platinum species with alumina. After calcination at 500°C, the *d–d* band at 355 nm was almost unchanged (with a minor shift to 350 nm). However, the 275 nm CT band disappeared and a new band at 230 nm was observed. If

TABLE 2

Electron Diffraction Pattern Analysis of the Support and of the Pt/Al_2O_3 (A3), Re/Al_2O_3 (B), and $Pt–Re/Al_2O_3$ (C4) Catalysts

Calculated *d*-spacings (Å)	Support Interplanar spacings (Å)	
	γ-Al_2O_3	TiO_2 (rutile)
2.241	$2.39_{(311)}$	
1.821	$1.977_{(400)}$	
1.435		$1.424_{(221)}$
1.312		$1.304_{(311)}$
1.079	$1.027_{(731)}$	$1.083_{(330)}$
0.928		$0.907_{(402)}$
0.809	$0.806_{(844)}$	

Calculated *d*-spacings (Å)	A3 Interplanar spacings (Å)	
	Pt	Pt_3Ti
3.237		$3.28_{(102)}$
2.241	$2.65_{(111)}$	$2.254_{(004)}$
1.942	$1.962_{(200)}$	
1.619		$1.637_{(204)}$
1.457		$1.434_{(106)}$
1.334		$1.376_{(220)}$
1.261		$1.270_{(206)}$
1.165	$1.183_{(311)}$	$1.153_{(126)}$
0.988	$0.981_{(400)}$	
0.910	$0.900_{(331)}$	

Calculated *d*-spacings (Å)	B Interplanar spacings (Å)
	$Al(ReO_4)_3$
3.15	3.17
2.842	2.76
2.590	2.545
1.975	1.967
1.689	1.695

Calculated *d*-spacings (Å)	C4 Interplanar spacings (Å)		
	Pt	Re	Pt_3Ti
2.601		$2.545_{(103)}$	
2.276	$2.265_{(111)}$		$2.254_{(004)}$
2.111		$2.105_{(101)}$	$2.109_{(202)}$
1.810			$1.814_{(005)}$
1.387	$1.387_{(220)}$		$1.380_{(110)}$
1.289		$1.270_{(206)}$	$1.262_{(103)}$
1.095	$1.133_{(222)}$	$1.114_{(004)}$	
1.033		$1.01_{(104)}$	
0.883	$0.877_{(420)}$	$0.885_{(211)}$	
0.790	$0.8008_{(422)}$		

TABLE 3

Results of Carbon Monoxide Isothermal Adsorption (μmol/g cat)

Sample	Total	Weakly adsorbed	Strongly adsorbed
A1	7.6	3.5	4.1
B	2.7	0.78	2
C1	13.1	2.5	10.6
C4	24.1	14.2	9.9

we take this band as a CT band of platinum, we can speculate that the platinum species on alumina was no longer a $[PtCl_6]^{2-}$ ion. The platinum must be in a more complex form; for example, a $[PtO_xCl_y]$ complex (4), or may be in another form which interacts with alumina or titania strongly. Since the characteristic absorption band of PtO_2 is at 350 nm and the *d–d* band of platinum also occurs at this wavelength, the existence of PtO_2 is possible.

Two reduction peaks of the Pt/Al_2O_3 catalysts were observed (Fig. 4). It is possible to assume that the 300°C peak is due to the reduction of PtO_2 species. The latter peak is attributed to the reduction of platinum species which interact strongly with the support or to the reduction of a surface complex (14). It is interesting to note that the temperature of the latter reduction peak shifts from 435 to 475°C when the platinum content decreases from 0.5 to 0.15 wt%. This result suggests that with less platinum content, the interaction of platinum with the support is stronger.

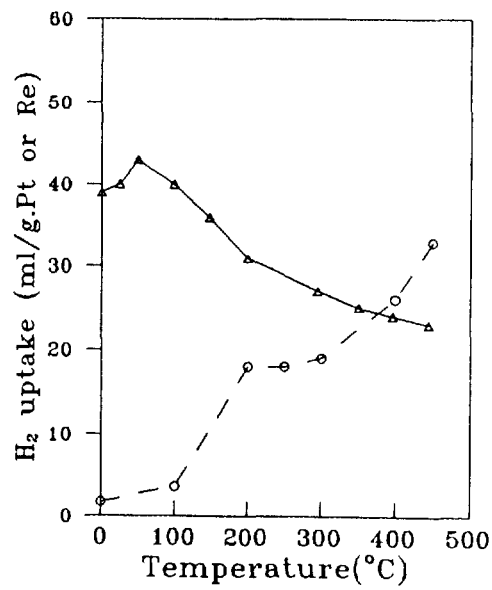

FIG. 8. Hydrogen adsorption isobars for the (—△—) Pt/Al_2O_3 and (—○—) Re/Al_2O_3 catalysts.

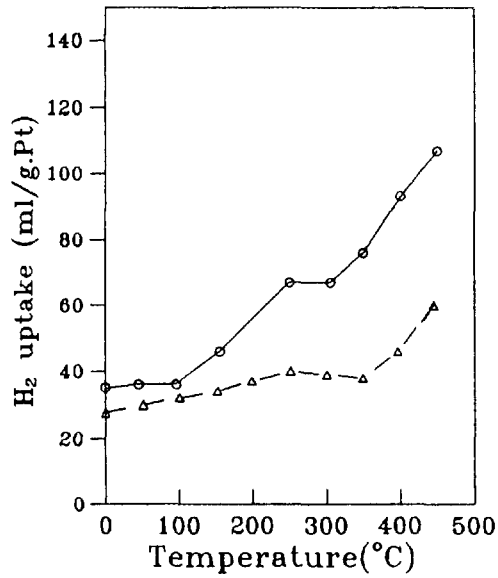

FIG. 9. Hydrogen adsorption isobars for the (—○—) C1 and (—△—) C4 catalysts.

SAED results show that metallic platinum and a Pt–Ti alloy are formed in the reduced Pt/Al_2O_3 catalyst. According to the DRS and TPR results, we can speculate that the metallic platinum results from the reduction of PtO_2 and the Pt–Ti alloy results from the reduction of a platinum species which strongly interact with titania in the support. The excess hydrogen consumption, compared to the reduction stoichiometry of $H_2/Pt = 1$, may correspond to the reduction of part of the titania. Furthermore, the formation of a Pt–Ti alloy may imply that the interaction between platinum species and the titania is stronger than that between platinum and alumina. The hydrogen adsorption isobar for the Pt/Al_2O_3 catalyst shows that the hydrogen uptake decreases when the temperature is raised. This probably results from the desorption of hydrogen at high temperatures.

Re/Al_2O_3 Catalyst

The UV absorption bands of $HReO_4$ solution are observed at 203 and 226 nm which agree well with literature data (15–17). The principal bands of the calcined Re/Al_2O_3 catalyst appear at 245 and 305 nm. These deviate greatly from those of $HReO_4$ solution. This may imply that the rhenium in the calcined Re/Al_2O_3 catalyst is no longer in the T_d symmetry of the ReO_4^- ion. This may indicate a strong interaction between the rhenium oxide and the support. Also, the possibility of the formation of some surface rhenium compounds cannot be excluded (18–20). No rhenium oxides were observed by SAED and this may be because any rhenium oxide formed after calcination of the catalyst was dissolved by the HF aqueous solution treatment. In addition, the formation of an $Al(ReO_4)_3$ complex and the absence of any rhenium titanium compound or Re–Ti alloy probably means that rhenium species interacted more strongly with alumina than with titania.

The Re/Al_2O_3 catalyst is more difficult to reduce compared to Pt/Al_2O_3. Two peaks with maximum reduction temperatures at 615 and 740°C are seen in the TPR spectrum. This indicates that the Re/Al_2O_3 catalyst cannot be properly reduced at the temperature used in industrial practice (about 500°C). This could be one of the reasons why the hydrogen adsorption and CO adsorption on the Re/Al_2O_3 catalyst are very low at low temperatures.

Almost no hydrogen adsorption takes place on Re/Al_2O_3 when the temperature is lower than 100°C. But it increases significantly when the temperature is above 100°C. This suggests that Re(0) can adsorb hydrogen at high temperatures. It is possible that the reduction of the remaining rhenium oxide takes place at high temperatures because Re/Al_2O_3 was not well reduced at low temperatures. The consumption of hydrogen due to this reduction may account for a part of the increase in hydrogen uptake at high temperatures on the Re/Al_2O_3 catalyst.

$Pt–Re/Al_2O_3$ Catalyst

The major absorption bands of the freshly prepared and dried catalyst (C1) are at 270, 350, and 450 nm (Fig. 2). These three bands are almost the same as the absorption bands of the dried Pt/Al_2O_3 catalyst, which is an indication of the existence of adsorbed $[PtCl_6]^{2-}$ ion. The rhenium in this dried catalyst did not exhibit its characteristic absorption bands; probably an interaction between $[PtCl_6]^{2-}$ and ReO_4^- is the reason. However, the possibility of the absorption bands overlapping with those of $[PtCl_6]^{2-}$ cannot be ruled out. The UV diffuse reflectance absorption data showed significant changes after the calcination of the Pt–Re catalyst. This result indicated that the catalyst phases changed after calcination. The 245 nm band can be attributed to Re(VII) (18). The presence of Re(VI) cannot be confirmed from our experiments (21). The diffuse reflectance spectra of $Pt–Re/Al_2O_3$ catalysts with $Re/Pt > 1$ are similar to that of Re/Al_2O_3 while the spectra of catalysts with $Re/Pt < 1$ resemble that of Pt/Al_2O_3 (Fig. 3). The first TPR peak was constant at about 300°C in spite of differences in the Re/Pt ratio because this peak represents the co-reduction of platinum and rhenium (22, 23). The TPR peak at 740°C became more prominent with the decrease of platinum content in the catalyst (Fig. 6). It is evident that the reduction of rhenium species was catalyzed by platinum. The hydrogen consumption results indicate that rhenium cannot be totally reduced from Re^{+7} to Re^0. Indeed, TPR results of Wagstaff and Prins (24)

showed that if the Re/Pt ratio was over 0.6, part of the rhenium could not be reduced under 500°C. Hence, the TPR peak at 740°C may result from the co-reduction of rhenium and the support. Metallic platinum and rhenium and Pt_3Ti alloy were formed in the reduced Pt–Re catalyst. The formation of a Pt–Re alloy cannot be ascertained by electron diffraction measurement. However, the formation of a Pt–Re alloy phase is very possible from the SAED results which are in accord with Vegard's law. It is interesting that no Al–Re complex or alloy is found in the Pt–Re catalyst. This phenomenon may be caused by the catalyzed reduction of rhenium by platinum. An alternative interpretation is that platinum prohibits the interaction of rhenium with alumina (14).

Re(0) is known to chemisorb CO strongly while Re^{4+} surface sites do not chemisorb CO (2). The amount of chemisorbed CO on the Pt–Re catalyst (both C1 and C4) is greater than the sum of those on the Pt/Al_2O_3 and Re/Al_2O_3 catalysts. One explanation is that more Re(0) was formed in the bimetallic catalyst as compared with the monometallic catalyst. The amount of CO chemisorbed on the high Re/Pt ratio catalyst (C1: CO/Pt + Re = 0.4) is greater than that on the low Re/Pt ratio catalyst (C4: CO/Pt + Re = 0.22). This indicates that the surface concentration of Re(0) on the C1 catalyst is higher than that on the C4 catalyst (25).

The hydrogen uptake is greatly enhanced by the addition of rhenium to Pt/Al_2O_3 and it increases with temperature. However, the increase with temperature is more significant for the high Re/Pt ratio catalyst than with the low Re/Pt catalyst. A higher Re(0) concentration partly accounts for this phenomenon, although electronic and geometric effects of rhenium on platinum and hydrogen spillover cannot be neglected. It is known that hydrogen adsorbed at high temperatures is capable of hydrogenating carbonaceous surface overlayers (26). This result may be helpful to the understanding of the higher stability of the skewed catalyst with a high Re/Pt ratio as compared with that of the balanced one (27, 28).

CONCLUSIONS

The structures of supported Pt, Re, and Pt–Re catalysts were characterized in the stages of impregnation, calcination, and reduction.

Pt/Al_2O_3 catalyst can be well reduced in hydrogen under 500°C. However, the reduction becomes difficult with a decrease in platinum content from 0.5 to 0.15 wt%. The hydrogen uptake on the reduced Pt/Al_2O_3 decreases with increasing temperature. A Pt–Ti alloy phase was found in the reduced Pt/Al_2O_3 catalyst from interaction with titania in the Al_2O_3 support.

Re/Al_2O_3 catalyst cannot be properly reduced under 500°C. ReO_4^- ions interact strongly with alumina after calcination of the catalyst. SAED results show that an $Al(ReO_4)_3$ complex was formed in the Re/Al_2O_3 catalyst.

For coimpregnated Pt–Re catalysts, the reduction of rhenium species was catalyzed by platinum but the catalyst could not be totally reduced if the Re/Pt ratio was too high. With a higher rhenium to platinum ratio, more rhenium remained unreduced. The DRS spectra resemble that of a Re/Al_2O_3 catalyst if the Re/Pt ratio is greater than 1 and they resemble that of Pt/Al_2O_3 if Re/Pt ratio is smaller than 1. Pt, Re, and Pt_3Ti alloy phases were observed on reduced Pt–Re catalysts. The hydrogen uptake at high temperatures increases with the increase of rhenium to platinum ratio.

ACKNOWLEDGMENTS

We thank Professor Dezheng Wang for some helpful discussions. We are grateful to Mr. Zenglin Liu and Mrs. Yongmin Gao for performing the SAED experiments.

REFERENCES

1. Kluksdahl, H. E., U. S. Patent 3,415,737 (1968).
2. Nacheff, M. S., Kraus, L. S., Ichikawa, M., Hoffman, B. M., Butt, J. B., and Sachtler, W. M. H., *J. Catal.* **106,** 263 (1987).
3. Bolivar, C., Charcosset, H., Frety, R., Parimet, M., and Tournayan, L., *J. Catal.* **45,** 163 (1976).
4. Malet, P., Munuera, G., and Caballero, A., *J. Catal.* **115,** 567 (1989).
5. Augustine, S. M., and Sachtler, W. M. H., *J. Catal.* **106,** 417 (1987).
6. Menon, P. G., and Froment, G. F., *J. Mol. Catal.* **25,** 59 (1984).
7. Johson, M. F. L., and Leroy, V. M., *J. Catal.* **35,** 434 (1974).
8. Peri, J. B., *J. Catal.* **52,** 144 (1978).
9. Freel, J., *Prepr. Pap.—Am. Chem. Soc. Div. Petrol. Chem.* **18**(1), 10 (1973).
10. Kelley, M. J., Fung, A. S., McDevitt, M. R., Tooley, P. A., and Gates, B. C., in "Microstructural Properties and Catalysis," Materials Research Society Symposium Proceedings, Vol. III, pp. 23–33. 1988.
11. Tauster, S. J., Fung, S. C., and Garten, R. L., *J. Am. Chem. Soc.* **100,** 170 (1978).
12. Lietz, G., Lieske, H., Spindler, H., Hanke, W., and Volter, J., *J. Catal.* **81,** 17 (1983).
13. Alerasool, S., Boecker, D., Rejai, B., and Gonzalez, R. D., *Langmuir* **4,** 1083 (1988).
14. Augustine, S. M., and Sachtler, W. M. H., *J. Catal.* **116,** 184 (1989).
15. Carrington, A., Schonland, D., and Symons, M. C. R., *J. Chem. Soc.*, 659 (1957).
16. Hindman, J. C., and Wehner, P., *J. Am. Chem. Soc.* **75,** 2869 (1953).
17. Bailey, N., Carrington, A., Lott, K. A. K., and Symons, M. C. R., *J. Chem. Soc.*, 290 (1960).
18. Edreva-Kardjieva, R. M., and Andreev, A. A., *J. Catal.* **94,** 97 (1985).
19. Li Wang and Hall, W. K., *J. Catal.* **82,** 177 (1983).
20. Freel, J., *Prepr. Pap.—Am. Chem. Soc. Div. Petrol. Chem.* **18**(1), 10 (1973).
21. Garland, M., Baiker, A., and Workaun, A., *Ind. Eng. Chem. Res.* **30,** 440 (1991).
22. Isaacs, B. H., and Petersen, E. E., *J. Catal.* **77,** 43 (1982).
23. Mieville, R. L., *J. Catal.* **87,** 437 (1984).

24. Wagstaff, N., and Prins, R., *J. Catal.* **59,** 434 (1979).
25. Grau, J. M., and Parera, J. M., *Appl. Catal.* **70,** 9 (1991).
26. Margitfalvi, J., Gobolos, S., Kwaysser, E., Hegedus, M., Nagy, F., and Koltai, L., *React. Kinet. Catal. Lett.* **24**(3–4), 315 (1984).
27. Larsen, P. A., *in* "Question and Answer Session Hydroprocessing" (H. Th. Rijnten and H. J. Lovink, Eds.), Ketjen Catalysts Symposium, AKZO Chemie Ketjen Catalysts, The Netherlands, p. 75. 1986.
28. Chen, L. Y., Ni, Y. Q., Zang, J. L., Lin, L. W., Luo, X. H., and Cheng, S., *Appl. Catal. A* **97,** 133 (1993).